

ARTICLE OPEN



Synergistic combination of information from ground observations, geostationary satellite, and air quality modeling towards improved PM_{2.5} predictability

Jinhyeok Yu¹, Chul H. Song¹, Dogyeong Lee¹, Sojin Lee^{1,10}, Hyun S. Kim¹, Kyung M. Han¹, Seohui Park², Jungho Im², Soon-Young Park^{1,11}, Moongu Jeon³, Vincent-Henri Peuch⁴, Pablo E. Saide⁵, Gregory R. Carmichael⁶, Jeeho Kim¹, Jhoon Kim⁷, Chang-Keun Song^{1,2}, Jung-Hun Woo⁸ and Seong-Hyun Ryu⁹

Concentrations of ambient particulate matter (such as PM_{2.5} and PM₁₀) have come to represent a serious environmental problem worldwide, causing many deaths and economic losses. Because of the detrimental effects of PM_{2.5} on human health, many countries and international organizations have developed and operated regional and global short-term PM_{2.5} prediction systems. The short-term predictability of PM_{2.5} (and PM₁₀) is determined by two main factors: the performance of the air quality model and the precision of the initial states. While specifically focusing on the latter factor, this study attempts to demonstrate how information from classical ground observation networks, a state-of-the-art geostationary (GEO) satellite sensor, and an advanced air quality modeling system can be synergistically combined to improve short-term PM_{2.5} predictability over South Korea. Such a synergistic combination of information can effectively overcome the major obstacle of scarcity of information, which frequently occurs in PM_{2.5} prediction systems using low Earth orbit (LEO) satellite-borne observations. This study first presents that the scarcity of information is mainly associated with cloud masking, sun-glint effect, and ill-location of satellite-borne data, and it then demonstrates that an advanced air quality modeling system equipped with synergistically-combined information can achieve substantially improved performances, producing enhancements of approximately 10%, 19%, 29%, and 10% in the predictability of PM_{2.5} over South Korea in terms of index of agreement (IOA), correlation coefficient (R), mean biases (MB), and hit rate (HR), respectively, compared to PM_{2.5} prediction systems using only LEO satellite-derived observations.

npj Climate and Atmospheric Science (2023)6:41; <https://doi.org/10.1038/s41612-023-00363-w>

INTRODUCTION

Particulate matter with aerodynamic diameters smaller than 2.5 μm (PM_{2.5}) has come to represent a serious societal issue in South Korea and China, because their ambient concentrations frequently exceed criteria concentrations, particularly during winter and spring seasons^{1,2}. Detrimental effects of PM_{2.5} on human health have been well recognized. High PM_{2.5} can lead to high occurrence rates of stroke, ischemic heart diseases (IHD), chronic obstructive pulmonary diseases (COPD), and lung cancer^{3,4}. Because of the human toxicity of high PM_{2.5}, the South Korean Ministry of Environment (KMoE) has been performing PM_{2.5} forecasts since 2014 for the purpose of promptly alerting South Korean citizens of hazy events as well as for preparing national emergency programs for reducing the emissions of air pollutants.

Many countries have developed and operated their own short-term air quality forecasting systems (refer to Supplementary Note 1). Among those operational short-term air quality forecasting systems, the ECMWF (European Centre for Medium-Range Weather Forecasts) in Europe and the NASA (National Aeronautics and Space Administration) Goddard center in USA have implemented global air quality forecasts including PM_{2.5} and ozone

predictions using the C-IFS (Integrated Forecasting System with Atmospheric Composition)⁵ and GEOS-Chem (Goddard Earth Observing System with Chemistry)⁶ models, respectively. Several other organizations are also releasing indices of global and regional air quality as well as PM_{2.5} on a daily basis, based on multi-model air quality simulations⁷. Air quality forecasts are now becoming an important part of our daily life, much like traditional weather forecasts.

Although air quality forecasts provide people with important information on air quality every day, people (particularly those in South Korea) have expressed high degrees of dissatisfaction with the accuracy of PM_{2.5} forecasts^{8,9}. Therefore, there is a strong need to improve the predictability of ambient PM_{2.5} in South Korean society. In this context, the current study deals with important issues of how to enhance the accuracy of air quality predictions. The focus in terms of air pollution in South Korea and northeast Asia is now on PM_{2.5}. We therefore will pay particular attention to PM_{2.5} in this study. However, we believe that strategies and methods to enhance PM_{2.5} predictability can also be applied to other ambient pollutants such as ozone and NO₂.

¹School of Earth Sciences & Environmental Engineering, Gwangju Institute of Science and Technology (GIST), Gwangju, Republic of Korea. ²Department of Urban & Environmental Engineering, Ulsan National Institute of Science and Technology (UNIST), Ulsan, Republic of Korea. ³School of Electrical Engineering & Computer Science, Gwangju Institute of Science and Technology (GIST), Gwangju, Republic of Korea. ⁴Copernicus Atmosphere Monitoring Service (CAMS), European Centre for Medium-Range Weather Forecasts (ECMWF), Reading, UK. ⁵Department of Atmospheric & Oceanic Sciences, University of California Los Angeles (UCLA), Los Angeles, CA, USA. ⁶Department of Chemical & Biochemical Engineering, The University of Iowa, Iowa City, IA, USA. ⁷Department of Atmospheric Sciences, Yonsei University, Seoul, Republic of Korea. ⁸Department of Civil & Environmental Engineering, Konkuk University, Seoul, Republic of Korea. ⁹Mirae Climate Company, Seoul, Republic of Korea. ¹⁰Present address: Department of Safety and Environmental Research, The Seoul Institute, Seoul, Republic of Korea. ¹¹Present address: Department of Science Education, Daegu National University of Education, Daegu, Republic of Korea. ✉email: chsong@gist.ac.kr

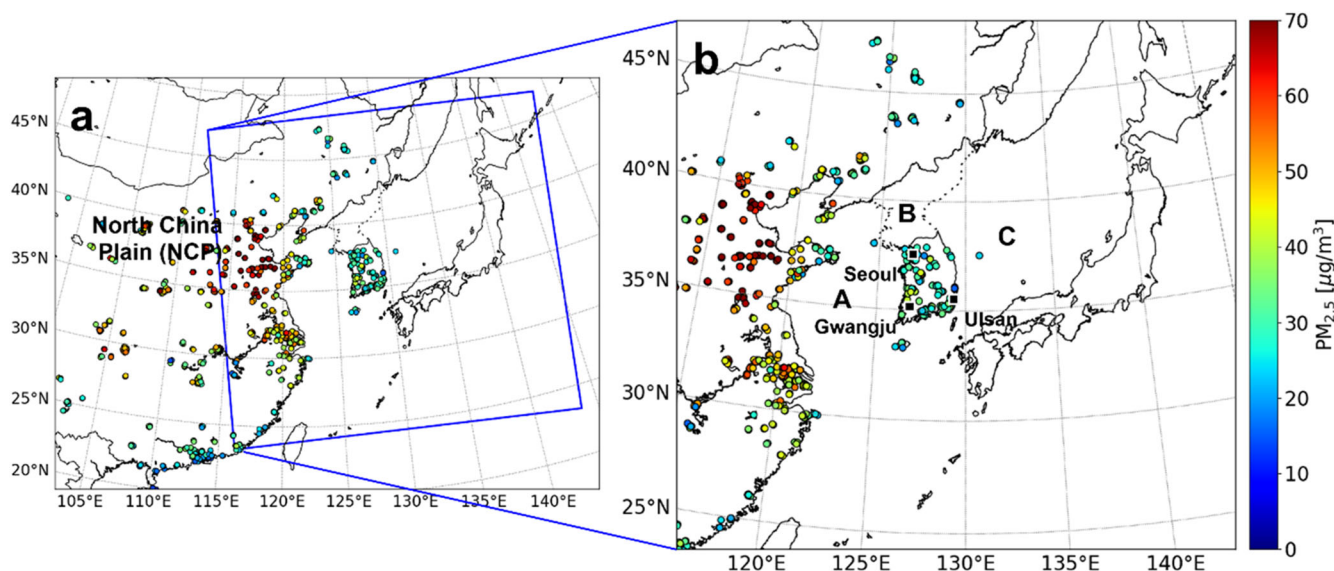


Fig. 1 Domains of this study. **a** Modeling domain and **b** GOCI domain. Circles in the two domains represent the locations of ground-observation stations inside China and South Korea. Color codes of the circles indicate averaged $PM_{2.5}$ during the KORUS-AQ campaign (between 1 May and 10 June, 2016). Regions A, B, and C are the Yellow Sea, North Korea, and the East Sea (or the Sea of Japan), respectively, where no surface $PM_{2.5}$ information is available. Further, the three black squares in panel **b** mark the locations of the three cities in South Korea where further analyses were conducted.

Throughout this study, several key data and ‘state-of-the-art’ technical elements are synergistically combined. Such key data and technical elements include: (i) aerosol data retrieved from Korean geostationary (GEO) satellite sensor; (ii) near real-time ground observations collected through a screen crawling technique; and (iii) outputs from an advanced air quality modeling system. The main objective of this study is to determine whether a smart combination of these technical elements and data could create synergy to improve $PM_{2.5}$ predictability over South Korea. All technical elements mentioned above were integrated into the framework of the K_AChEMS v2.0 (Korean Air Chemistry Modeling System version 2.0). The K_AChEMS v2.0 is an air quality modeling system that is currently being developed, primarily to enhance the predictability of $PM_{2.5}$ and PM_{10} in South Korea (for details on K_AChEMS v2.0, refer to the Methods and Supplementary Note 2). Figure 1 illustrates the domain of interest in this study.

RESULTS AND DISCUSSION

ECMWF CAMS_nrt products over South Korea

First, we start our discussion with CAMS_nrt (Copernicus Atmospheric Modeling and Monitoring Service, near real-time products), which is global air quality forecast data produced by the C-IFS of the ECMWF (for details on the C-IFS model simulations, see Supplementary Note 3)¹⁰.

Figure 2a presents hourly variations of averaged $PM_{2.5}$ over South Korea during the period of KORUS-AQ campaign (Korea–United States Air Quality campaign) carried out between 1 May, 2016 and 10 June, 2016. Figure 2 also shows comparisons between $PM_{2.5}$ predictions and $PM_{2.5}$ observations. $PM_{2.5}$ observations were acquired from a ground observation network in South Korea called ‘AIR KOREA’ that is managed by the KMoE. In Fig. 2, model-predicted $PM_{2.5}$ was based on averages of $PM_{2.5}$ at the grid cells corresponding to the locations of AIR KOREA stations over South Korea. This KORUS-AQ campaign has been well-investigated in terms of meteorological and physico-chemical characteristics^{11,12}. Therefore, we selected this campaign period as a time-window for this study.

The CAMS_nrt $PM_{2.5}$ in Fig. 2a shows a moderate agreement with observed $PM_{2.5}$, with an IOA (Index of Agreement) of 0.51.

Here, the IOA was calculated based on hourly $PM_{2.5}$ data. In addition, only IOA was presented in Fig. 2. However, other statistical metrics including errors and biases were also analyzed in Supplementary Note 4. This moderate IOA of 0.51 in Fig. 2a might be affected by two main factors: (i) modeling errors produced by C-IFS model simulations and (ii) imprecision in the initial state caused by data assimilation with LEO (low Earth orbit) satellite-derived data.

First, to evaluate the accuracy of C-IFS model simulations, we compared the predicted concentrations of major $PM_{2.5}$ constituents with observed concentrations of sulfate, organic aerosols (OAs), black carbon (BC), and dust at six intensive measurement stations in South Korea. The comparisons are shown in Supplementary Note 5. In general, C-IFS model simulations tended to over-predict dust and BC concentrations while under-predicting OA concentrations. These inaccuracies contributed to the moderate IOA shown in Fig. 2a. In addition, the relatively coarse resolution of the C-IFS model simulations (approximately $80 \times 80 \text{ km}^2$) can contribute to model errors.

Second, the precision of the initial states prepared by data assimilation are also crucial, particularly for short-term (i.e., one or two days) predictions. The CAMS_nrt system employs a 4-D VAR (4-Dimensional Variational) data assimilation method with MODIS (Moderate-resolution Imaging Spectro-radiometer) AOD (Aerosol Optical Depth)¹³. This 4-D VAR data assimilation method is a technique that can correct errors of model fields (background fields) with observations (near true value). Corrected fields (analysis fields) created by data assimilation are applied to operational C-IFS runs for initial conditions. Observational data for the 4-D VAR assimilation are AOD data retrieved from two MODIS sensors onboard Terra and Aqua satellites.

However, MODIS sensors (or other LEO UV/VIS sensors) have shown two serious limitations in terms of their data availability. First, they cannot produce AOD data over areas where clouds are present. We call this phenomenon ‘cloud masking’. For example, (north)east Asia is highly cloudy compared to other continents, mainly because of both large presences of cloud seeds (atmospheric aerosols) and high humidity. Such large cloud masking tends to lead to a large loss of aerosol data over (north)east Asia. In actuality, the average percentage of MODIS AOD data available

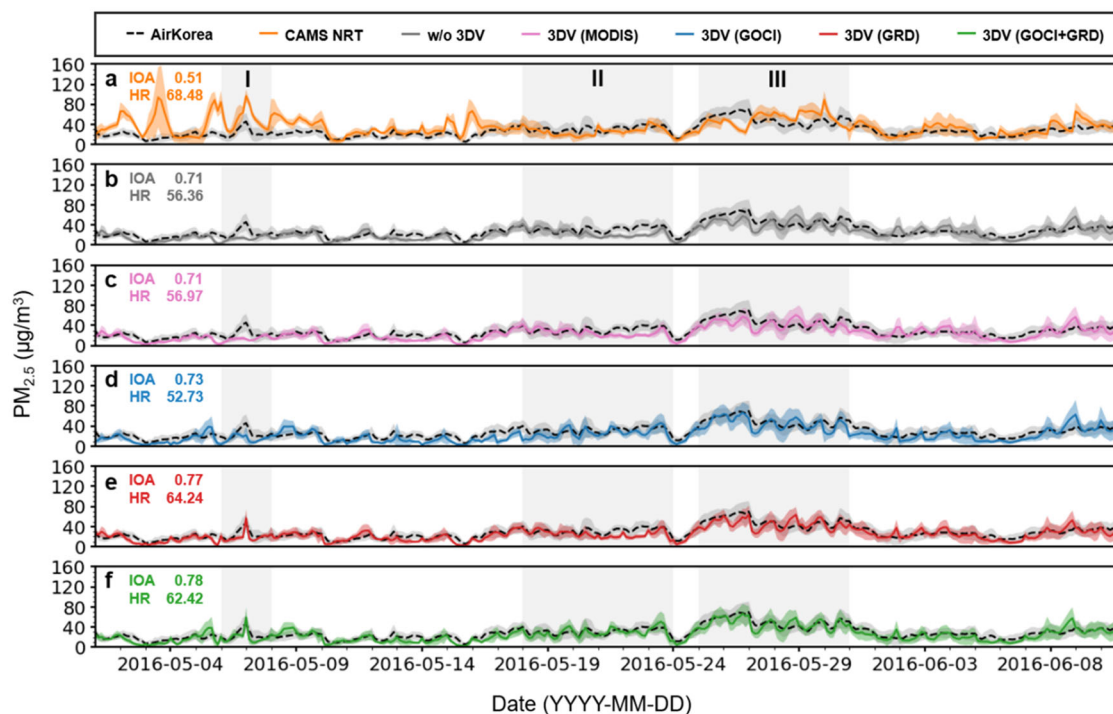


Fig. 2 Hourly variations of ground-observed and predicted $PM_{2.5}$ in South Korea. All $PM_{2.5}$ values inside South Korea are aggregated in the plots. **a–f** present comparisons between observed $PM_{2.5}$ and predicted $PM_{2.5}$ obtained in the experiments **a** from CAMS NRT, **b** from the control run (without 3DV), **c** with 3DV using MODIS AOD, **d** with 3DV using GOCI AOD, **e** with 3DV using ground observations, and **f** with 3DV using both GOCI AOD and ground observations. The color shadows around $PM_{2.5}$ represent ranges of one standard deviation of averaged $PM_{2.5}$. Two representative model performance metrics of IOA (scientific metrics) and HR (administrative metrics) are inserted into the plots. Other performance metrics are analyzed and listed in Supplementary Fig. 1. Here, IOAs were calculated based on hourly data at AIR KOREA stations. The three gray-shaded areas represent Asian dust (I), air stagnant (II), and long-range transport (III) episodes, respectively.

during the period of the KORUS-AQ campaign was only ~14% over the domain shown in Fig. 1.

Second, the results of monitoring via these two MODIS sensors are prone to be affected by the ‘sun-glint effect’. This is an inherent effect caused by the geometry between LEO satellite sensors and the sun. Because of the sun-glint effect, we sometimes lose many potentially important data, particularly over ocean areas, where no surface $PM_{2.5}$ observations are available¹⁴. This loss of MODIS AOD data due to the sun glint effect is discussed further in Supplementary Note 6.

Collectively, these two limitations in monitoring data from MODIS sensors result in a scarcity of AOD data or data related to $PM_{2.5}$. This scarcity of observed data can prevent data assimilation from effectively correcting model background errors. The moderate IOA of 0.51 shown in Fig. 2a is due to both modeling errors and the scarcity of the observations used in the data assimilation. In addition, Fig. 2a provides a typical example of how difficult accurate short-term $PM_{2.5}$ prediction is with our current levels of knowledge and techniques.

LEO vs. GEO satellite sensors

With lessons from CAMS_nrt, we set up a strategy to build up a more accurate short-term $PM_{2.5}$ prediction system over South Korea by developing a more advanced air quality modeling system intended to reduce modeling errors and by utilizing better satellite-borne $PM_{2.5}$ data to improve initial states^{15,16}. Regarding the former, we have developed K_AChEMS v2.0. Regarding the latter, we decided to use AOD products from the state-of-the-art Korean geostationary satellite sensor named GOCI (Geostationary Ocean Color Imager) instead of the two MODIS sensors. Although the GOCI sensor cannot also produce AOD data over pixels where

clouds are present, it can overcome the limitation of the sun-glint effect because it is a GEO satellite sensor.

Figure 2b is produced from K_AChEMS v2.0 without performing data assimilation (i.e., without updated initial conditions). With this effort alone, the IOA jumped up from 0.51 (Fig. 2a) to 0.71 (Fig. 2b), indicating the potential importance of the performance of the air quality modeling system. Figure 2c presents $PM_{2.5}$ predictions made by the K_AChEMS v2.0 with 3-D VAR (3-Dimensional Variational) data assimilation using only MODIS AOD. The experiment of Fig. 2c was a mimicking simulation of CAMS_nrt. Surprisingly, the IOA in Fig. 2c was the same as that in Fig. 2b. This was because MODIS AOD data were too sparse to affect the $PM_{2.5}$ predictability in South Korea due to both cloud masking and sun-glint effects. Again, the data coverage of MODIS sensors was only ~14%. With this low data coverage, the data assimilation appears to be almost ‘useless’.

This problem of data scarcity can be avoided in part by using GOCI satellite-retrieved AOD. When we used GOCI-retrieved AOD data, the percentage of the AOD data available during the period of the KORUS-AQ campaign over the monitoring domain of the GOCI increased up to 28.5%. Here, we attempted to use AOD products from the Korean GOCI sensor in 3-D VAR data assimilation. Figure 2d presents the $PM_{2.5}$ predictability from this experiment. Enhancements in $PM_{2.5}$ predictability can be seen visually in Fig. 2 as well as in terms of IOA. The IOA again increased from 0.71 to 0.73, showing that assimilation of GOCI AOD data could more effectively correct model errors in the initial state than MODIS AOD data.

III-location of information: satellite data vs. ground observations

Despite the substantial advancements that have been made, both MODIS- and GOCI-retrieved data have inherent and unavoidable

disadvantages: ‘data scarcity’ and ‘data ill-location’. As mentioned above, the average percentage of the GOCI AOD data available over the entire GOCI domain was approximately 28.5%. This means that we could not obtain AOD data from 71.5% of GOCI pixels, mainly due to the presence of clouds. The presence of clouds is the major reason for the problem of scarcity of satellite-borne aerosol data. In addition, even 28.5% of the GOCI aerosol data are not always available at useful locations for PM_{2.5} predictions in South Korea. For example, if some portions of GOCI AOD data are available over areas where air masses cannot influence air quality in South Korea (e.g., over the northern edges of the modeling domain or over the East China Sea, which is far from the Korean peninsula), then such AOD data become meaningless in terms of their ability to improve PM_{2.5} predictability in South Korea. We refer to this type of problem as the ‘ill-location problem’ of satellite data.

To overcome the problems of data scarcity and data ill-location, we must return back to classical observation data, i.e., ground observations. Because ground observations are being made at fixed surface locations, these data are never affected by the presence of clouds. Figure 1 shows PM_{2.5} measurement networks in China (at approximately 1800 locations) and in South Korea (at approximately 400 sites)^{17,18}. However, a challenging point is whether we can obtain these observation data in near real-time. In the case of ‘past’ observations, they can be downloaded from the data archive. However, it is difficult to collect ‘present’ data in a near real-time mode. To resolve this problem, we decided to develop a method called the ‘screen crawling technique’ (also known as the ‘scraping technique’)¹⁹. Using this digital software technique, we can scan and obtain observation data from corresponding Chinese and Korean websites in a near real-time (in situ) mode. Such near real-time observations can then be utilized almost immediately in the PM_{2.5} prediction system after a quick data quality inspection called the ‘buddy test’, which was described in detail in Lee et al.²⁰.

Figure 2e shows how large improvements in PM_{2.5} predictions over South Korea can be achieved by assimilating ground PM_{2.5} observations instead of GOCI AODs. The IOA increased from 0.73 to 0.77. We could also find additional advantages by assimilating the data of these ground observations. In Fig. 2, the gray-shadow period I was characterized as an ‘Asian dust episode’ that had taken place from 6 May to 7 May, 2016. During this period, dust plumes were generated in the Inner Mongolia, and they were then transported long distance over northeastern China and the Yellow Sea. Unfortunately, these dust plumes were not detected by the GOCI sensor because such dust plumes are frequently co-present with cold frontal clouds. However, the ground observation network inside China certainly detected these dust plumes. During dust episodes, PM₁₀ exhibits a tendency to increase, because dust particles are predominantly composed of coarse-mode particles (i.e., particles larger than 2.5 μm). In this study, we assimilated both ground PM_{2.5} and PM₁₀ (refer to Supplementary Note 7). Supplementary Fig. 6e clearly shows that our prediction could also capture the dust peak in PM₁₀ during period I. By contrast, PM₁₀ predictions in Supplementary Fig. 6d, wherein only GOCI products were assimilated, could not capture the dust peak.

Such enhancements in PM_{2.5} predictability via the assimilation of ground PM_{2.5} are also presented in Supplementary Fig. 1 and summarized in Table 1. The assimilation of ground PM_{2.5} exhibits larger impacts on PM_{2.5} predictability than the assimilation of GOCI products. Again, the limited effects of the assimilation of GOCI products are attributable to their scarcity and undesirable locations. This is the most compelling reason to assimilate ‘ground’ PM_{2.5} and PM₁₀ to enhance PM_{2.5} and PM₁₀ predictability.

Table 1. Summary of scientific and administrative statistical metrics for all of South Korea, Seoul, Gwangju, and Ulsan.

	IOA	R	RMSE ¹	MB ¹	ACC ²	HR ²
All of South Korea						
CAMS NRT	0.51	0.27	24.67	7.11	49.64	68.48
w/o 3DV	0.71	0.52	16.81	−4.56	57.53	56.36
3DV (MODIS)	0.71	0.53	16.67	−4.26	58.82	56.97
3DV (GOCI)	0.73	0.56	17.54	−5.04	55.38	52.73
3DV (GRD)	0.77	0.60	15.11	−3.30	66.57	64.24
3DV (GOCI + GRD)	0.78	0.63	15.25	−3.04	65.28	62.42
Seoul (37.6° N, 126.9° E)						
CAMS NRT	0.53	0.31	25.50	11.27	36.59	63.64
w/o 3DV	0.71	0.52	17.55	−3.02	48.78	45.45
3DV (MODIS)	0.71	0.52	17.55	−3.02	48.78	45.45
3DV (GOCI)	0.71	0.51	17.51	−2.66	48.78	45.45
3DV (GRD)	0.76	0.59	16.07	−2.23	60.98	54.55
3DV (GOCI + GRD)	0.76	0.60	15.94	−3.24	65.85	45.45
Gwangju (35.2° N, 126.8° E)						
CAMS NRT	0.40	0.13	28.01	11.31	46.34	60.00
w/o 3DV	0.75	0.63	14.55	−7.12	65.85	40.00
3DV (MODIS)	0.75	0.63	14.55	−7.12	65.85	40.00
3DV (GOCI)	0.77	0.63	14.48	−6.92	65.85	40.00
3DV (GRD)	0.77	0.62	14.68	−4.71	60.98	40.00
3DV (GOCI + GRD)	0.80	0.68	13.08	−4.76	65.85	50.00
Ulsan (35.6° N, 129.3° E)						
CAMS NRT	0.53	0.27	23.78	3.47	48.78	54.55
w/o 3DV	0.76	0.62	17.83	0.63	80.49	90.91
3DV (MODIS)	0.76	0.62	17.83	0.63	80.49	90.91
3DV (GOCI)	0.76	0.62	17.81	0.97	80.49	90.91
3DV (GRD)	0.77	0.67	18.51	3.58	80.49	81.82
3DV (GOCI + GRD)	0.79	0.67	16.47	1.96	85.37	90.91

¹ Unit: μgm^{−3}; ² Unit: %.

What if ground and satellite-derived observations are used together?

What can happen if ground PM_{2.5} observations and GOCI-borne data are used together for data assimilation? Can we expect a synergism? To answer this question, we designed one more experiment with sequential data assimilation of ground PM_{2.5} and GOCI AOD; Fig. 2f shows the results of this case study. As shown in Fig. 2f, the IOA increased again from 0.77 to 0.78 over the entire period of the KORUS-AQ campaign, implying that the addition of either GOCI-derived AOD into ground PM_{2.5} could improve the precision of the initial state and thus the PM_{2.5} predictability throughout South Korea.

This appears to be particularly true for the two gray-shadow periods II and III in Fig. 2. Gray-shadow periods II and III were characterized by KORUS-AQ scientists as ‘a period of air stagnation’ and ‘an episode of long-range transport’ from China, respectively. During the period of air stagnation (between 18 May and 23 May, 2016), an anticyclone sat around the Korean peninsula. Because of this, air masses were rotating clockwise with low wind speeds around the Korean peninsula (see Fig. 3b). This low-speed rotation of air masses created a favorable condition for air pollutants to be accumulated around the Korean peninsula. On the other hand, during the period of long-range transport (between 25 May and 30 May, 2016), air pollutants, including PM_{2.5}, were transported long distance from the North

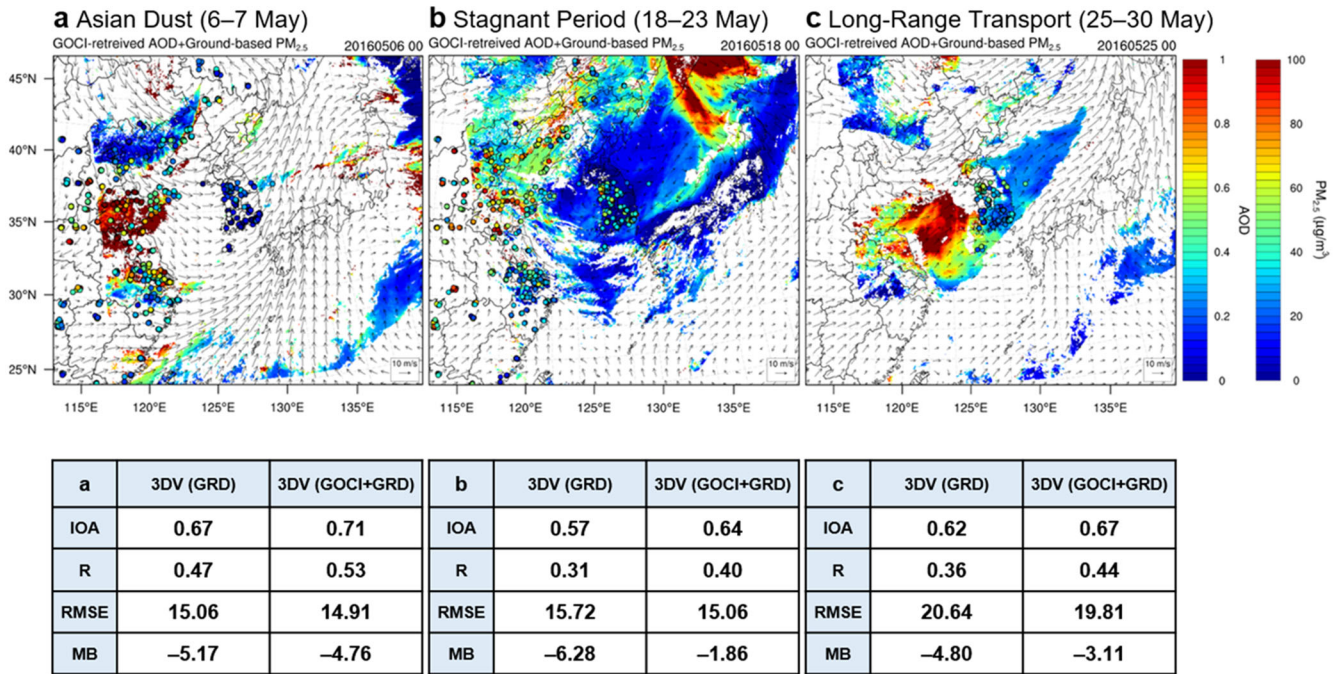


Fig. 3 Three representative plots showing how effective geostationary satellite-derived information can be to enhance $PM_{2.5}$ predictability in South Korea. **a** Asian dust episode, **b** air stagnant episode, and **c** long-range transport episode took place on 6–7 May, 18–23 May, and 25–30 May, respectively, during the period of the KORUS-AQ campaign. It should also be noted that, in all three cases, GOCI AOD data were available over upwind areas of South Korea. Wind vectors shown with arrows were obtained at 850 hPa.

China Plain (NCP) to South Korea due to strong westerlies (see Fig. 3c). We found that $PM_{2.5}$ increased up to $60 \mu\text{g}/\text{m}^3$ on 26 May, 2016. As can be seen visually in Fig. 2f, the gaps between $PM_{2.5}$ observations and predictions during these two gray periods became narrower than those in Fig. 2e. A similar situation was also found for the predictions of PM_{10} , as shown in Supplementary Fig. 6f. These results are particularly important, because both air stagnation and long-range transport are two typical meteorological conditions under which the levels of $PM_{2.5}$ in the Korean peninsula are frequently enhanced. If the situation is really like this one, then the following question arises: what factor creates such improvements in $PM_{2.5}$ and PM_{10} predictability?

The answer to this question is presented in Fig. 3, which demonstrates a synergism created by sequential data assimilation using ground $PM_{2.5}$ observations and GOCI-derived AOD. During the periods II and III, sequential applications of both forms of data to data assimilation allowed IOA to jump up from 0.57 to 0.64 during the period of air stagnation and from 0.62 to 0.67 during the period of long-range transport. In case of air stagnation, GOCI AOD data were available over the Yellow Sea (denoted as A in Fig. 1), North Korea (denoted as B in Fig. 1), and the East Sea (denoted as C in Fig. 1). This data availability was due to the fact that the sky was very clear (uncloudy) as a result of the anticyclone located around the Korean peninsula. Because of the rotation of air masses, all the three regions became upwind regions to South Korea in this case. Therefore, it is crucial to have information over all three of these regions to achieve accurate $PM_{2.5}$ predictions in South Korea.

The episode of long-range transport (period III) is another excellent example regarding the creation of synergism. Surprisingly, during this period, ground $PM_{2.5}$ measurements inside China were all turned off. However, high AOD plumes were detected by the GOCI sensor over the Yellow Sea. The Yellow Sea was an upwind region to South Korea in this case (see the arrows of winds in Fig. 3c). In addition to the ground $PM_{2.5}$ information available inside South Korea, the GOCI AOD data available over the Yellow

Sea helped us further enhance the accuracy of $PM_{2.5}$ predictions in South Korea.

Over the entire period of the KORUS-AQ campaign, including the two episodes discussed above, our advanced $PM_{2.5}$ prediction system (Fig. 2f) exhibited enhancements of approximately 10%, 19%, 29%, and 10% in the predictability of $PM_{2.5}$ over South Korea, in terms of IOA, R (Pearson correlation coefficient), MB (mean biases), and HR (hit rate), respectively, compared to the $PM_{2.5}$ prediction system using LEO-retrieved observations alone (Fig. 2c) (for details, also refer to Supplementary Fig. 1 and Supplementary Note 4).

Although this study paid particular attention to the predictions of ‘surface’ $PM_{2.5}$, using both GOCI AOD and ground $PM_{2.5}$ in the data assimilation was also found to be extremely helpful in analyzing the aerosol concentrations ‘above the surface’. Supplementary Fig. 7 in Supplementary Note 8 presents the comparison of vertical profiles between observed and predicted aerosol concentrations. As shown in Supplementary Fig. 7, the experiment using GOCI AOD and ground $PM_{2.5}$ exhibited the highest agreements with aircraft-borne aerosol observations, even above the surface.

Blank area of information

As described above, South Korea is surrounded by so-called ‘blank areas of information’ such as the Yellow Sea, North Korea, and the East Sea. However, transboundary air pollution events from China to South Korea are almost always occurring through these blind regions along the strong persistent westerly and/or northwesterly winds. This means that, for improved $PM_{2.5}$ (and PM_{10}) predictability in South Korea, it is certainly necessary to have information on air quality over these blind regions.

In this context, we demonstrated that information from GEO satellite sensors over those blank areas of information could help us substantially improve $PM_{2.5}$ predictability in South Korea. Although it is true that geostationary satellite data can help us improve PM predictability, there is no 100% guarantee that GEO

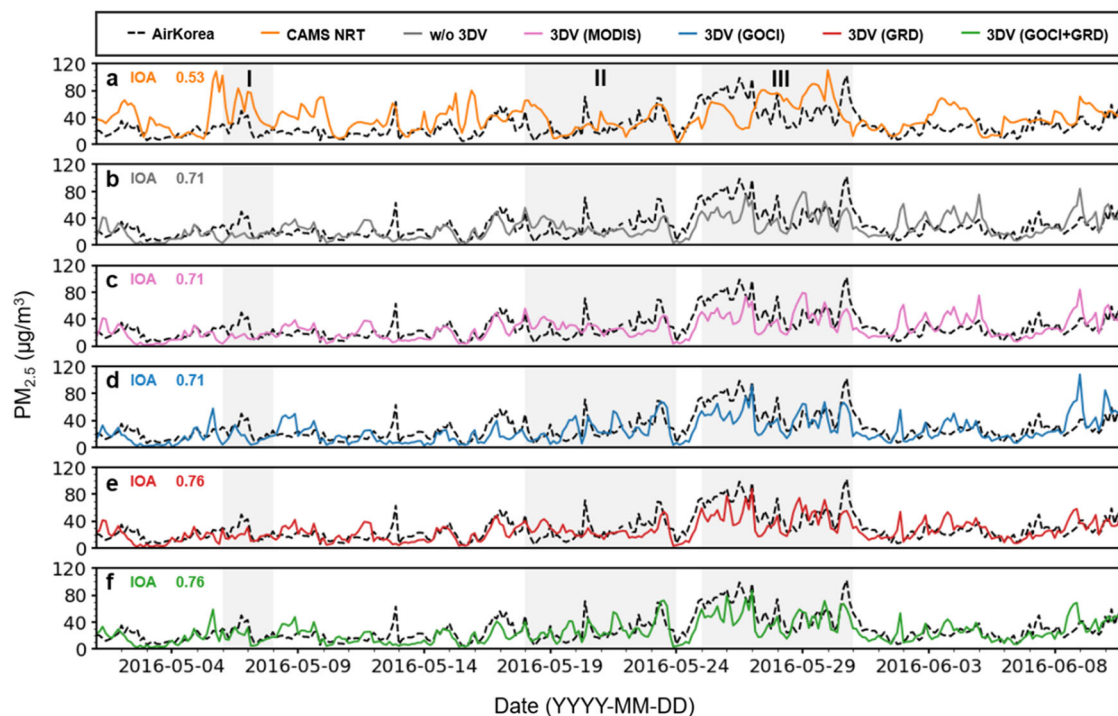


Fig. 4 Hourly variations of ground-observed and predicted $PM_{2.5}$ in Seoul. Panels **a–f** present comparisons between observed $PM_{2.5}$ and predicted $PM_{2.5}$ obtained in the experiments **a** from CAMS NRT, **b** from the control run (without 3DV), **c** with 3DV using MODIS AOD, **d** with 3DV using GOCI AOD, **e** with 3DV using ground observations, and **f** with 3DV using both GOCI AOD and ground observations. The three gray-shaded areas represent Asian dust (I), air stagnant (II), and long-range transport (III) episodes, respectively.

satellite data are always available over the blank areas due to the random presence of clouds. To provide more convincing data availability over the blank regions, it would be helpful to establish surface observation networks to boost the performances of $PM_{2.5}$ predictions in South Korea. The establishment of a surface observation network may be a cheaper and more guaranteed way to improve $PM_{2.5}$ predictability in South Korea than launching expensive GEO satellite sensors.

Based on the discussions shown above, establishing several air quality monitoring towers or stations above the Yellow Sea and the East Sea as well as inside North Korea will be highly useful for achieving better $PM_{2.5}$ predictions in South Korea. Of course, building air monitoring stations inside the territory of North Korea would create political arguments. It appears to be a difficult task to achieve politically, although it is an easy task to accomplish technically.

Additional analyses and discussion

In this work, we have evaluated the performances of K_AChEMS v2.0 at the country-level. To more closely scrutinize the performances of K_AChEMS v2.0, we have evaluated the performance of K_AChEMS v2.0. To further assess its performance, we zoomed into three key areas inside South Korea: Seoul, Gwangju (located in the southwest of South Korea), and Ulsan (located in the southeast of South Korea) (see Fig. 1 for the locations of these three cities). We have then further assessed the performances of K_AChEMS v2.0 in these three cities. Table 1 summarizes the $PM_{2.5}$ predictability of K_AChEMS v2.0 in those three cities in South Korea. In addition, Fig. 4 shows a similar analysis to Fig. 1 for Seoul.

Based on the results presented in Fig. 4 and Table 1, it can also be seen that the conclusions drawn from our investigations in the three cities are similar to those drawn from our investigations over all of South Korea. For example, we again see increased IOAs from 0.71 (Fig. 4b) to 0.76 (Fig. 4f) in Seoul. The results from the

Gwangju and Ulsan studies also show similar trends to those from the country-level investigations (refer to Table 1).

In this study, we have reported our major findings inferred from experiments during the period of the KORUS-AQ campaign. To more firmly support our conclusions, we also carried out another six-month test-bed experiment between 1 November, 2016 and 30 April, 2017 (a high $PM_{2.5}$ period in South Korea). Test results from this six-month investigation are discussed in Supplementary Note 9. In short, we again drew the same conclusions from the six-month experiment. Based on this finding, we now believe that our conclusions drawn from this study are general ones, not period-specific. The methods and strategies applied to South Korea can also be applied to many other regions that encounter similar situations. In this sense, our methods and strategies are not area-specific, either.

IOAs and other statistical metrics such as root mean square errors, mean biases, and so on are commonly used in the science community. We refer to these metrics as ‘scientific statistical metrics’. On the other hand, the HR is a metric that administration parties such as KMoE are taking particular care of in South Korea. Because of this, we refer to the HR as an ‘administrative statistical metric’. The HR is defined as the percentage of successful hits of category intervals of $PM_{2.5}$ in South Korean air quality standards (refer to Supplementary Note 10 for a detailed equation for HR calculation). However, high IOAs do not always guarantee high HRs, because HR is estimated based on the hit percentage of category intervals. Although we believe the HR is less scientific, there has also been a strong requirement to enhance the HR in South Korea. This was why we also inserted HRs into Fig. 2. It could be seen that HRs increased continuously from Fig. 2b–f. There are several more administrative statistical metrics such as ACC (Accuracy), POD (Probability of detection), and FAR (False alarm rate), and definitions of these metrics can be found in Supplementary Note 10. Among these administrative statistical

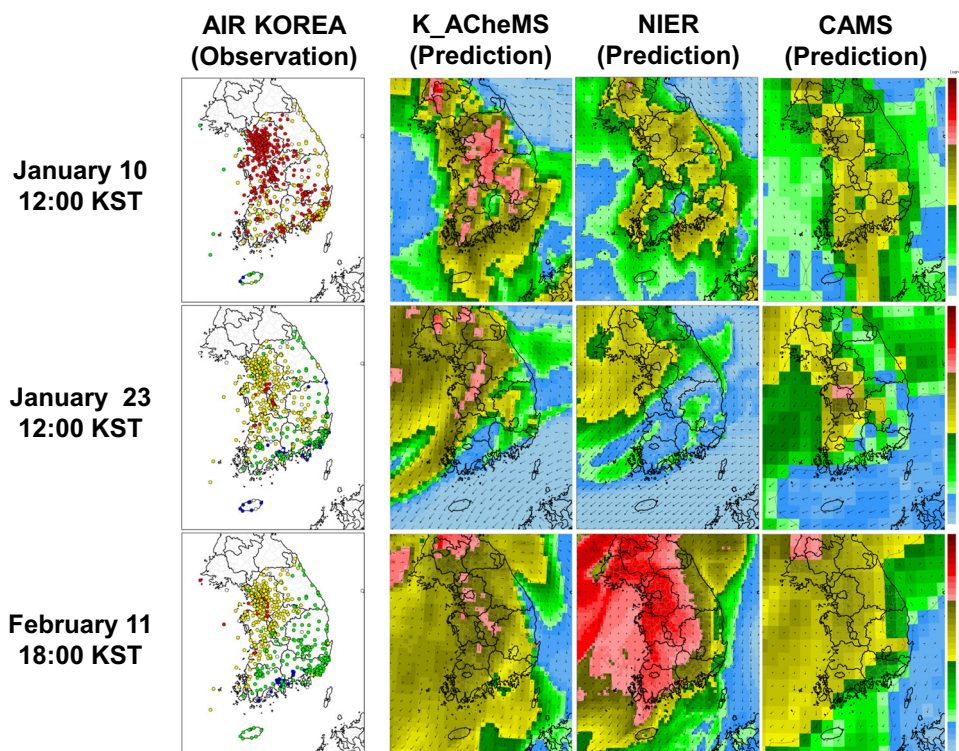


Fig. 5 Performances of K_ACheMS v2.0 for PM_{2.5} predictions over South Korea. The first column presents levels of observed PM_{2.5} from AIR KOREA, while the second, the third, and the fourth columns respectively present PM_{2.5} predictions from K_ACheMS v2.0 and two operational PM_{2.5} prediction systems at NIER and ECMWF. Red, yellow, green, and blue colors indicate ‘very bad (very unhealthy)’, ‘bad (unhealthy)’, ‘moderate’, and ‘good’ air qualities, respectively, in terms of Korean PM_{2.5} standards. The PM_{2.5} prediction service using operational K_ACheMS v2.0 was launched on 1 Jan., 2022 and has been operated continuously since then. The first, second, and third rows are PM_{2.5} observations and predictions taken at noon on 10 Jan., 23 Jan., and 11 Feb., 2022, respectively.

metrics, both the ACC and HR for our experiments are summarized in Table 1.

Model performances for operational runs. The K_ACheMS v2.0 discussed in this study has been run for operational PM_{2.5} predictions over South Korea since 1 Jan., 2022 (visit website at <https://kachems.gist.ac.kr>). Figure 5 presents the parts of performances of the K_ACheMS v2.0 through comparisons between PM_{2.5} observations and PM_{2.5} predictions. In Fig. 5, three PM_{2.5} predictions from the K_ACheMS v2.0, current operational PM_{2.5} prediction systems at NIER (National Institute of Environmental Research in South Korea) and ECMWF are compared with PM_{2.5} observations from AIR KOREA. The PM_{2.5} predictions from the NIER have been based on a different approach of an ensemble average of 20 outputs from 20 combinations among different meteorology, air quality models and emission inventories⁸. It can be seen in Fig. 5 that the K_ACheMS v2.0 produced much better PM_{2.5} predictions than the other two systems for three major high PM_{2.5} episodes. The three high PM_{2.5} episodes shown in Fig. 5 were the biggest ones that occurred over the six months, during which the K_ACheMS v2.0 were operated.

During the six-month test period, the IOA and HR from the K_ACheMS v2.0 were 0.78 and 67%, respectively. These numbers were substantially higher than those produced by the ECMWF prediction system (IOA: 0.76 and HR: 54%). Although the PM_{2.5} predictions from the NIER system were not released yet, the annual averaged HR of the NIER system has been reported to be approximately 55–60%. Further analyses regarding the operation runs of K_ACheMS v2.0 are made in Supplementary Note 11 (refer to Supplementary Tables 6 and 7). Based on these analyses, the new PM_{2.5} prediction system proposed in this study appears to have been working very well.

METHODS

K_ACheMS v2.0

K_ACheMS v2.0 consists of the following: (i) Chemistry-transport model (CMAQ vG, a CMAQ model significantly modified by Gwangju Institute of Science and Technology in South Korea); (ii) Meteorological models including the WRF-ARW (Advanced Research version of the Weather and Research Forecasting) model and UK Met Office UM (Unified Model), together with WRF-MCIP (Meteorology-Chemistry Interface Processor) and UM-MCIP; (iii) bottom-up emissions based on KORUS v5.0; (iv) data assimilation system based on 3-D VAR and EnKF (Ensemble Kalman Filter) methods using ground observations and/or geostationary GOCI; and (v) machine learning elements such as XGBoost (eXtreme Gradient Boost)²¹. Each element of the K_ACheMS v2.0 is described further in Supplementary Note 2.

In the current study, the horizontal resolution for K_ACheMS v2.0 was set at $15 \times 15 \text{ km}^2$ for northeast Asia, and there were 15 vertical layers from the surface to 50 hPa. The chemical initial conditions for the K_ACheMS v2.0 were updated at every 00 UTC via assimilation with GOCI AODs and/or ground PM_{2.5} measured at 00 UTC. 24–48 h air quality predictions were then carried out using the updated initial conditions.

The CMAQ vG (Community Multi-scale Air Quality version G) model has been actively developed based on the US EPA CMAQ v5.2 model²². In particular, the model has been improved through the following additions: (i) daytime HONO photo-chemistries²³, (ii) heterogeneous HO₂ reactions²⁴, (iii) gas- and aqueous-phase halogen chemistries²⁵, and (iv) new yield data for the formation of secondary organic aerosols acquired from multiple smog chamber experiments conducted under typical conditions of northeast

Asia²⁶. These new additions will be discussed in other publications.

For anthropogenic emissions, KORUS v5.0 has been used. KORUS v5.0 is a bottom-up emission inventory that was specifically established for the KORUS-AQ campaign²⁷. K_AChEMS v2.0 uses two meteorological fields generated by WRF-ARW model²⁸ and UM²⁹. This study used the meteorological fields generated via WRF-ARW model using $0.25^\circ \times 0.25^\circ$ -resolved NOAA GFS MET fields for initial and boundary conditions.

Two data assimilation techniques have been developed and incorporated into K_AChEMS v2.0: the 3-D VAR and EnKF methods. Although the EnKF method has outperformed the 3-D VAR method in our PM_{2.5} predictions³⁰, we decided to use the 3-D VAR method in the present study. The 3-D VAR method has been shown to have several limitations compared to the EnKF technique. For example, its background error information is relatively simple and not flow-dependent. It also has a lack of temporal propagation. However, when using of the EnKF technique, we typically generate 30–40 ensemble members to construct background error covariance matrices, which means that operational runs of K_AChEMS v2.0 using the EnKF technique would require approximately 30–40 times larger hardware resources than those of K_AChEMS v2.0 using the 3-D VAR method. Due to the strong concern of high computation costs, we decided to employ the 3-D VAR technique in the operation runs of K_AChEMS v2.0.

Data assimilation methods

To use the 3-D VAR method, we had to develop background and observation error covariance matrices. To update the initial conditions, data assimilations were carried out at every 00 UTC with satellite-borne and/or ground observations. Further technical details regarding the 3-D VAR method can be found in Supplementary Note 12.

DATA AVAILABILITY

The data are available upon request to the corresponding author.

Received: 5 October 2022; Accepted: 3 May 2023;

Published online: 23 May 2023

REFERENCES

- Kim, H. C. et al. Recent increase of surface particulate matter concentrations in the Seoul Metropolitan Area, Korea. *Sci. Rep.* **7**, 4710 (2017).
- Huang, R.-J. et al. High secondary aerosol contribution to particulate pollution during haze events in China. *Nature* **514**, 218–222 (2014).
- Apte, J. S., Marshall, J. D., Cohen, A. J. & Brauer, M. Addressing global mortality from ambient PM_{2.5}. *Environ. Sci. Technol.* **49**, 8057–8066 (2015).
- Burnett, R. T. et al. An integrated risk function for estimating the global burden of disease attributable to ambient fine particulate matter exposure. *Environ. Health Perspect.* **122**, 397–403 (2014).
- Flemming, J. et al. Tropospheric chemistry in the integrated forecasting system of ECMWF. *Geosci. Model Dev.* **8**, 975–1003 (2015).
- Keller, C. A. et al. Description of the NASA GEOS composition forecast modeling system GEOS-CF v1.0. *J. Adv. Model. Earth Syst.* **13**, e2020MS002413 (2021).
- For example, to find a global and regional multi-model air quality forecasts, go to <http://waqi.info/forecast/#/> (January 11, 2023).
- Chang, L.-S. et al. Human-model hybrid Korean air quality forecasting system. *J. Air Waste Manag. Assoc.* **66**, 896–911 (2016).
- Koo, Y.-S., Kim, S.-T., Cho, J.-S. & Jang, Y.-K. Performance evaluation of the updated air quality forecasting system for Seoul predicting PM₁₀. *Atmos. Environ.* **58**, 56–69 (2012).
- <https://apps.ecmwf.int/datasets/data/macc-nrealtime/> (January 11, 2023).
- Peterson, D. A. et al. Meteorology influencing springtime air quality, pollution transport, and visibility in Korea. *Elementa-Sci. Anthropol.* **7**, 57 (2019).

- Kim, H., Zhang, Q. & Heo, J. Influence of intense secondary aerosol formation and long-range transport on aerosol chemistry and properties in the Seoul Metropolitan Area during spring time: results from KORUS-AQ. *Atmos. Chem. Phys.* **18**, 7149–7168 (2018).
- Benedetti, A. et al. Aerosol analysis and forecast in the European Centre for medium-range weather forecasts integrated forecast system: 2. Data assimilation. *J. Geophys. Res.-Atmos.* **114**, D13205 (2009).
- Cox, C. & Munk, W. Measurement of the roughness of the Sea Surface from photographs of the Sun's glitter. *J. Opt. Soc. Am.* **44**, 838–850 (1954).
- Lee, S. et al. GIST-PM-Asia v1: development of a numerical system to improve particulate matter forecasts in South Korea using geostationary satellite-retrieved aerosol optical data over Northeast Asia. *Geosci. Model Dev.* **9**, 17–39 (2016).
- Lee, K. et al. Development of Korean Air Quality Prediction System version 1 (KAQPS v1) with focuses on practical issues. *Geosci. Model Dev.* **13**, 1055–1073 (2020).
- Go to <http://www.cnemc.cn/en> for China urban air quality real-time data release platform (January 11, 2023).
- Go to <https://www.airkorea.or.kr> for AIR KOREA (January 11, 2023).
- Singrodia, V., Mitra, A. & Paul, S. A review on web scrapping and its applications. in *2019 International Conference on Computer Communication and Informatics (ICCCI)* 1–6 (2019). <https://doi.org/10.1109/ICCCI.2019.8821809>.
- Lee, S. et al. Impacts of uncertainties in emissions on aerosol data assimilation and short-term PM_{2.5} predictions over Northeast Asia. *Atmos. Environ.* **271**, 118921 (2022).
- Chen, T. & Guestrin, C. XGBoost: A Scalable Tree Boosting System. in *Proceedings of the 22nd ACM SIGKDD International Conference on Knowledge Discovery and Data Mining* 785–794 (Association for Computing Machinery, 2016). <https://doi.org/10.1145/2939672.2939785>.
- Byun, D. & Schere, K. L. Review of the governing equations, computational algorithms, and other components of the models-3 community multiscale air quality (CMAQ) modeling system. *Appl. Mech. Rev.* **59**, 51–77 (2006).
- Zhang, L. et al. Potential sources of nitrous acid (HONO) and their impacts on ozone: a WRF-Chem study in a polluted subtropical region. *J. Geophys. Res. Atmos.* **121**, 3645–3662 (2016).
- Macintyre, H. L. & Evans, M. J. Parameterisation and impact of aerosol uptake of HO₂ on a global tropospheric model. *Atmos. Chem. Phys.* **11**, 10965–10974 (2011).
- Sarwar, G. et al. Impact of enhanced ozone deposition and halogen chemistry on tropospheric ozone over the northern hemisphere. *Environ. Sci. Technol.* **49**, 9203–9211 (2015).
- Babar, Z. B., Park, J.-H., Kang, J. & Lim, H. Characterization of a Smog chamber for studying formation and physicochemical properties of secondary organic aerosol. *Aerosol. Air Qual. Res.* **16**, 3102–3113 (2016).
- Woo, J.-H. et al. Development of the CREATE inventory in support of integrated climate and air quality modeling for Asia. *Sustainability* **12**, 7930 (2020).
- Skamarock, C. et al. A Description of the Advanced Research WRF Model Version 4.1. (2019) <https://doi.org/10.5065/1dfh-6p97>.
- Brown, A. et al. Unified modeling and prediction of weather and climate: a 25-year journey. *Bull. Am. Meteorol. Soc.* **93**, 1865–1877 (2012).
- Park, S.-Y. et al. Implementation of an ensemble Kalman filter in the Community Multiscale Air Quality model (CMAQ model v5.1) for data assimilation of ground-level PM_{2.5}. *Geosci. Model Dev.* **15**, 2773–2790 (2022).

ACKNOWLEDGEMENTS

This research was supported by the National Research Foundation of Korea (NRF) grant funded by the Ministry of Science and ICT (MSIT) (Nos. 2020M3G1A1114617, 2020M3G1A1114621, and 2021R1A2C1006660).

AUTHOR CONTRIBUTIONS

J.Y., D.L., K.M.H., and S.-Y.P. carried out K_AChEMS model simulations and data analysis; S.L., P.E.S., and G.R.C. established data assimilation technique; H.S.K., M.J., S.P., J.I., and J.K. developed machine learning techniques; V.-H.P. provided ECMWF CAMS data; J.K. and C.-K.S. developed GOCI AOD retrieval algorithm; J.-H.W. prepared emissions; S.-H.R. developed screen crawling technique; C.H.S. designed and supervised research and wrote the paper.

COMPETING INTERESTS

The authors declare no competing interests.

ADDITIONAL INFORMATION

Supplementary information The online version contains supplementary material available at <https://doi.org/10.1038/s41612-023-00363-w>.

Correspondence and requests for materials should be addressed to Chul H. Song.

Reprints and permission information is available at <http://www.nature.com/reprints>

Publisher's note Springer Nature remains neutral with regard to jurisdictional claims in published maps and institutional affiliations.



Open Access This article is licensed under a Creative Commons Attribution 4.0 International License, which permits use, sharing, adaptation, distribution and reproduction in any medium or format, as long as you give appropriate credit to the original author(s) and the source, provide a link to the Creative Commons license, and indicate if changes were made. The images or other third party material in this article are included in the article's Creative Commons license, unless indicated otherwise in a credit line to the material. If material is not included in the article's Creative Commons license and your intended use is not permitted by statutory regulation or exceeds the permitted use, you will need to obtain permission directly from the copyright holder. To view a copy of this license, visit <http://creativecommons.org/licenses/by/4.0/>.

© The Author(s) 2023